

Quantum-classical correspondence and mechanical analysis of a classical-quantum chaotic system*

Haiyun Bi(毕海云)^{1,3}, Guoyuan Qi(齐国元)^{2,†}, Jianbing Hu(胡建兵)¹, and Qiliang Wu(吴启亮)⁴

¹School of Mechanical Engineering, Tiangong University, Tianjin 300384, China

²Tianjin Key Laboratory of Advanced Technology of Electrical Engineering and Energy, Tiangong University, Tianjin 300384, China

³The Key Laboratory of Advanced Perception and Intelligent Control of High-end Equipment, Ministry of Education, and School of Mathematics and Physics, Anhui Polytechnic University, Wuhu 241000, China

⁴Post-doctorate Research Station of Mechanical Engineering, School of Electrical Engineering and Automation, Tiangong University, Tianjin 300384, China

(Received 27 October 2019; revised manuscript received 4 December 2019; accepted manuscript online 16 December 2019)

Quantum-classical correspondence is affirmed via performing Wigner function and a classical-quantum chaotic system containing random variables. The classical-quantum system is transformed into a Kolmogorov model for force and energy analysis. Combining different forces, the system is divided into two categories: conservative and non-conservative, revealing the mechanical characteristic of the classical-quantum system. The Casimir power, an analysis tool, is employed to find the key factors governing the orbital trajectory and the energy cycle of the system. Detailed analyses using the Casimir power and an energy transformation uncover the causes of the different dynamic behaviors, especially chaos. For the corresponding classical Hamiltonian system when Planck's constant $\hbar \rightarrow 0$, the supremum bound of the system is derived analytically. Difference between the classical-quantum system and the classical Hamiltonian system is displayed through trajectories and energies. Quantum-classical correspondences are further demonstrated by comparing phase portrait, kinetic, potential and Casimir energies of the two systems.

Keywords: quantum, Wigner function, Hamiltonian system, force and energy transformation

PACS: 05.45.-a, 05.45.Mt

DOI: 10.1088/1674-1056/ab6205

1. Introduction

Research on quantum applications has attracted a great deal of attention recently, especially in quantum computation,^[1] quantum chip,^[2] quantum communication, quantum application in image binarization^[3] using quantum entanglement^[4] or quantum protocols,^[5] and so on. Quantum mechanics does not describe the phase space of the system motion as classical mechanics because of the uncertainty and stochasticity. However, quantum systems become classical Hamiltonian systems in the limit when Planck's constant $\hbar \rightarrow 0$.^[6] Alternatively, researchers have demonstrated that under decoherence a quantum system corresponds to a conservative chaotic Hamiltonian system. In the last two decades, researchers have investigated the correspondence between quantum and classical Hamiltonian systems. For example, Brack *et al.*^[7] demonstrated the existence of quantum beats in a classical system, i.e., the Hénon–Heiles system, which is a conservative chaotic Hamiltonian system. Hou and Hu^[8] as well as Song *et al.*^[9,10] derived the relationship between quantum entanglement and classical chaos through the average linear entropy using the Dicke Hamiltonian model. Eckhardt *et al.*^[11] presented a conservative chaotic Hamiltonian function in which there appears quantum mechanical behavior. Gong

and Brumer^[12] pointed out that the decoherence, i.e., the loss of coherence, of a quantum system corresponds to this conservative chaotic Hamiltonian system. Taking into account the quantum-classical correspondence, the classical chaotic system is called a classical-quantum chaotic system. Furthermore, researchers examined the classical-quantum correspondence in the chaotic system using a uniform structure measure for the distribution functions of both the classical and quantum phase spaces.^[13] When the ratio of two parameters in the chaotic system is large, the maximum Lyapunov exponent is larger than that of many other existing conservative chaotic systems, such as the classical Hénon–Heiles system.^[7] Therefore, the objective of this paper is the study of the classical-quantum chaotic system, particular in relation to the quantum mechanics of decoherence and study of corresponding classical Hamiltonian conservative system in the limit when Planck's constant $\hbar \rightarrow 0$.

Chaotic systems mainly divide into two major categories: dissipative systems for which the divergence of the system is less than zero and conservative systems for which it is equal to zero.^[14,15] Conservative systems preserve the volume in phase space, its dimension being integer, whereas dissipative systems do not conserve the volume, its dimension being fractional. From the Liouville theorem, a Hamiltonian system

*Project supported by the National Natural Science Foundation of China (Grant Nos. 61873186 and 11902220), the Natural Science Foundation of Tianjin City of China (Grant No. 17JCZDJC38300), the Provincial Foundation for Excellent Young Talents of Colleges and Universities of Anhui Province of China (Grant No. GXYQ2017014), and the Anhui University Humanities and Social Sciences Research Project of China (Grant No. SK2019A0116).

†Corresponding author. E-mail: guoyuanqisa@qq.com

must conserve this volume.^[16] Hence, the conservative chaotic Hamiltonian system is restricted more than the conservative chaotic non-Hamiltonian system, because it conserves both Hamiltonian energy and volume. To our knowledge, research on the conservative chaos dynamics is scant, especially concerning the conservative chaotic Hamiltonian systems.

More and more researchers pay attention to nonlinear dynamic analyses,^[17–20] especially dynamic analyses of chaotic systems. The methodologies employed entail numerical calculations, analyses of boundaries, aperiodic solutions, sensitivity to initial, bifurcation,^[21–24] circuit implementation,^[25] Lyapunov exponent calculations,^[26,27] fractional order,^[28] Melnikov analysis,^[29–33] Poincaré map,^[34,35] system control, and synchronization.^[36] Both the Melnikov method and the mechanical analysis method divide a Hamiltonian system with disturbance into a conservative part and a non-conservative part, similarities between the two methods are corresponding to the conservative part, the rate of change of the Melnikov function in the Melnikov method and the Casimir function of the mechanical analysis method are both zeros. The Melnikov function is analyzed from a mathematical perspective, and the Casimir function has a physical background. The Melnikov method uses the homoclinic orbit to find the existence conditions of chaos in the sense of Smale horseshoe. The mechanical analysis method first obtains the extreme surface and then analyze trajectory characteristics of the system via extreme surface. Other methods also do not cover the mechanics of the chaotic systems such as the conservation of energy, the physical underpinnings and background, the conversion among the internal energy, the dissipation, and the external force. Recently, Pelino *et al.*,^[37] Qi *et al.*,^[38,39] Yang and Qi^[40] have studied the mechanics including energy transformation, force for some chaotic systems. For instance, using the Kolmogorov model, Pelino *et al.*^[37] presented the energy cycle of the Lorenz system. For the brushless dc motor chaotic system, Qi^[38] decomposed the forces and derived the energy cycling by employing the Kolmogorov model and the Casimir function. Using the mechanics analysis method, Yang and Qi^[40] decomposed the vector field of the plasma chaotic system into four types of torque: inertial, internal, dissipative, and external, and comparison of mechanics analysis and generalized competitive mode analysis. For the chaotic system of a permanent-magnet synchronous motor, the Casimir energy as stored energy and its rate of change as the power difference between the dissipative energy and the energy supplied to the motor are employed to shed some insight into the mechanisms of the system.^[39] Moreover, details of mechanical analysis or energy cycling of many chaotic systems are revealed by converting these systems into the Kolmogorov form.^[41–45] The mechanical analysis is able to uncover the causes of sinks, periodic orbits, and chaos produced by systems. However,

studies concerning the mechanism have only focused on dissipative chaotic systems. To date, there has been no analysis of causes of different dynamical behaviors for a quantum, classical-quantum or conservative Hamiltonian system.

A classical-quantum chaotic Hamiltonian system can display both classical chaotic and quantum features. Therefore, the mechanical analysis is a good technique to uncover the mechanism behind the production of different dynamical behaviors.

This paper identifies a classical-quantum chaotic system and quantum-classical correspondence as the object of study. The classical-quantum chaotic system is transformed into a Kolmogorov-type system characterized by a vector field of three forces: inertial, internal, and external. Correspondingly, three energies, i.e., kinetic, potential and supplied, are found for the classical-quantum Hamiltonian system. The mechanism behind the dynamical behaviors, such as periodic orbits, pseudo-periodic orbits, sources and chaos, are revealed using a combination of forces and energy. The Casimir power is employed to find the cause for the different dynamical behaviors. For the corresponding classical Hamiltonian system, the supremum bound of the system is derived analytically and a variety of dynamics is shown in the Lyapunov spectrum. By comparing trajectories and energies of the system, difference between the classical-quantum system and the classical Hamiltonian system is demonstrated. Quantum-classical correspondences are demonstrated by comparing trajectories, 3D view of the phase space trajectories, phase portrait, energies of the two systems.

The structure of this paper is as follows. In Section 2, the quantum-classical correspondence is conducted and the corresponding classical Hamiltonian system is described. In Section 3, the classical-quantum system is transformed into an equivalent Kolmogorov-type system. The Casimir power is used to further reveal the cause of each orbit type, especially chaotic flow. In Section 4, quantum-classical correspondences are further displayed via energies. A summary is given in Section 5.

2. Quantum-classical correspondence and classical Hamiltonian system

In this study, the classical Hamiltonian function chosen to investigate the corresponding quantum mechanical system is^[11–13]

$$H(\mathbf{Y}) = \frac{1}{2}(p_x^2 + p_y^2) + \frac{a}{2}x^2y^2 + \frac{b}{4}(x^4 + y^4), \quad (1)$$

where a and b are parameters, x and y the system coordinates with corresponding system momenta p_x and p_y , $\mathbf{Y} = [x, y, p_x, p_y]^T$. For this system, the corresponding time-

independent Schrödinger equation is

$$\left[-\frac{\hbar^2}{2}\nabla^2 + \frac{a}{2}x^2y^2 + \frac{b}{4}(x^4 + y^4)\right]\psi = E\psi, \quad (2)$$

where \hbar is Planck's constant, ψ the wave function, and ∇^2 the Laplace operator. In rectangular coordinates, the gradient operator is $\nabla = \frac{\partial}{\partial x}i + \frac{\partial}{\partial y}j$. The operators x , p_x , y , and p_y satisfy the commutation relations $[x, p_x] = i\hbar$, $[x, p_y] = 0$, $[y, p_x] = 0$, $[y, p_y] = i\hbar$.

For convenience, let $x_1 = x$, $x_2 = y$, $x_3 = p_x$, $x_4 = p_y$, then $H(\mathbf{X})$ can be rewritten as

$$H(\mathbf{X}) = \frac{1}{2}(x_3^2 + x_4^2) + \frac{a}{2}x_1^2x_2^2 + \frac{b}{4}(x_1^4 + x_2^4), \quad (3)$$

where \mathbf{X} is a vector, $\mathbf{X} = [x_1, x_2, x_3, x_4]^T$.

In the quantum world, the notion of a certain point in the phase space does not make sense because the positions x_1 and x_2 , the momenta x_3 and x_4 cannot be measured instantly (Heisenberg's uncertainty principle). To describe the behavior of quantum, we have to introduce a function of quasi-probability density, called the Wigner function, to measure the random property of quantum state. The Wigner function has a good performance for analyzing quantum unstable variables, and is written as

$$W_{mn} = \frac{1}{(\pi\hbar)^2} \exp\left(-\frac{(x_1^2 + x_2^2 + x_3^2 + x_4^2)}{\hbar}\right) \times L_m\left(\frac{2}{\hbar}(x_1^2 + x_3^2)\right) L_n\left(\frac{2}{\hbar}(x_2^2 + x_4^2)\right), \quad (4)$$

where the Laguerre polynomial $L_k(x) = \frac{e^x}{k!} \frac{d^k}{dx^k} (e^{-x}x^k)$.

The Wigner function of a given state can be calculated by Eqs. (3) and (4) with fixed $m = n = 5$.

The Wigner distribution is presented in Figs. 1(a) and 1(b) with respect to the planes of $x_1 - x_3$ and $x_2 - x_4$, respectively. The classical phase space has probability density being real and normalized. However, differing from the probability density, the Wigner function does not have to be positively definite. No matter what the energy is, the phase space has regions where the Wigner function takes on negative values, as shown in Figs. 1(a) and 1(b). These figures in 3D look like the ripples of water. Further, to clearly see the characteristics of distribution, the contour plots are displayed in Figs. 1(b) and 1(c), which demonstrate two properties of the Wigner function: (1) high and low scattered wave form, (2) uniform distribution to any direction like concentric circles. The Wigner function is shown with respect to one coordinate [Fig. 1(e)]. Interestingly, the trend of the distribution of Wigner with the variable x_3 (same for other variables) is very similar to the sampling function^[46] $F(\omega) = 2\text{Sa}(\omega) = 2\sin \omega / \omega$ [Fig. 1(f)], which reflects the frequency spectrum distribution of a rectangular pulse.

The Wigner function is employed to calculate the mean of quantum behavior or trajectory $\langle x_i \rangle$ based on the Hamiltonian equation. Equation (5) governs how the Wigner function impacts the behavior of quantum. The arbitrary quantum state can be acquired via

$$\langle m|f(\mathbf{X})|n\rangle = \int f(\mathbf{X})W_{mn}(\mathbf{X})d\mathbf{X}. \quad (5)$$

Symbol $\langle * \rangle$ indicates the mean of variable $*$.

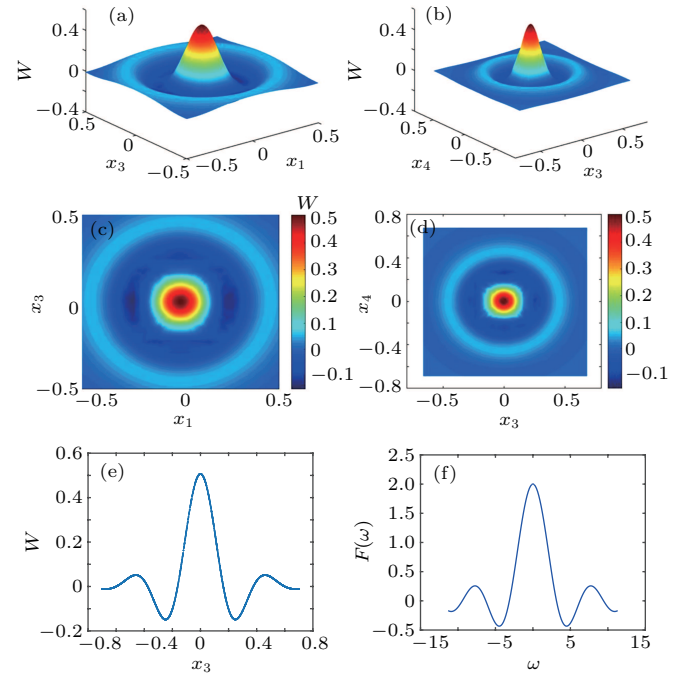


Fig. 1. The Wigner distribution in 3D space: (a) (x_1, x_3, W) and (b) (x_2, x_4, W) , 2D plane: (c) (x_1, x_3) and (d) (x_2, x_4) , (e) $W-x_3$, (f) frequency spectrum of the rectangular pulse signal.

Eckhardt *et al.*^[11] studied a quantum mechanics of the corresponding Hamiltonian function (1) in observations of scars, periodic orbits, and vibrational adiabaticity. Corresponding to Hamiltonian function (1), in order to exhibit the random property and keep the classical Hamiltonian equation, Gong and Brumer^[12] gave the following system

$$\begin{aligned} dx &= \frac{\partial H}{\partial p_x} dt, \\ dy &= \frac{\partial H}{\partial p_y} dt, \\ dp_x &= -\frac{\partial H}{\partial x} dt + \sqrt{2D}\eta_1, \\ dp_y &= -\frac{\partial H}{\partial y} dt + \sqrt{2D}\eta_2, \end{aligned} \quad (6)$$

where D is the energy-dependent rate from the environment, η_1 and η_2 are the independent real differential stochastic variables. The classical Hamiltonian function, Eq. (3), is selected for three reasons: (a) the energy scaling is sufficient to avoid any overwhelming energy exchange with the environment under quantum condition, (b) the chaotic degree is sufficient to

recognize the classical-quantum discrepancy, and (c) the potential has no simple harmonic terms.^[11]

Furthermore, the quantum-classical corresponding to the Hamiltonian function (3) is examined for the conservative chaotic Hamiltonian system using a uniform structure measure for the distribution functions of the quantum and classical phase space.^[13] However, through literature review, there has been no literature concerning a mechanical analysis related to forces and energy conversions and the evolutionary dynamics of the classical-quantum systems.

By Eq. (3) and $x_1 = x, x_2 = y, x_3 = p_x, x_4 = p_y$, we have $\frac{\partial H}{\partial p_x} = \frac{\partial H}{\partial x_3} = x_3, \frac{\partial H}{\partial p_y} = \frac{\partial H}{\partial x_4} = x_4, -\frac{\partial H}{\partial x} = -\frac{\partial H}{\partial x_1} = -ax_1x_2^2 - bx_1^3, -\frac{\partial H}{\partial y} = -\frac{\partial H}{\partial x_2} = -ax_1^2x_2 - bx_2^3$, system (6) is rewritten as

$$\begin{aligned} \dot{x}_1 &= x_3, & \dot{x}_2 &= x_4, \\ \dot{x}_3 &= -ax_1x_2^2 - bx_1^3 + \sqrt{2D}\eta_1, \\ \dot{x}_4 &= -ax_1^2x_2 - bx_2^3 + \sqrt{2D}\eta_1. \end{aligned} \quad (7)$$

The general classical system refers to the system corresponding to quantum system in the limit when Planck's constant

$\hbar \rightarrow 0$. At this time, there is decoherence between the classical system and the quantum system, which has been studied by many scholars, such as Ref. [12]. From Eq. (5), the integration makes the state trajectory generated by Hamiltonian equation smoother, or less random, however, because of the randomness of Wigner function, the quantum trajectory still exhibits chaotic. This counteraction makes the decoherence between classical and quantum normally under the condition $\hbar \rightarrow 0$. Therefore, our paper discuss the correspondence between a new classical system (7) containing random terms and the quantum system, which is also the significance of this paper. For the sake of clarity, we call system (7) the classical-quantum system corresponding to quantum systems of Hamiltonian function (3) with Wigner function (4).

Because the dynamics of quantum system is quite hard to investigate, we can firstly confirm whether the stochastic dynamical behavior of system (7) reflects the stochastic behavior of the quantum system. This can be verified by finding the correspondence of the means of both the quantum system and the classical-quantum system (7).

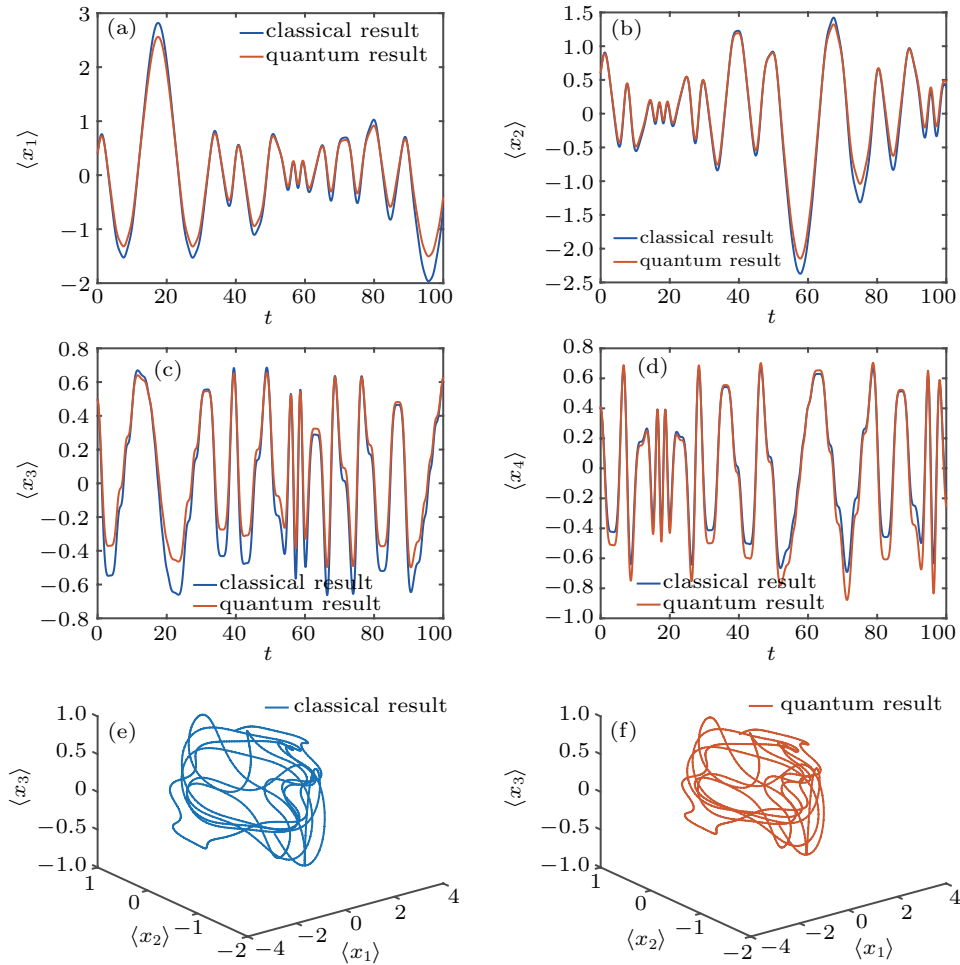


Fig. 2. Time series for (a) $\langle x_1 \rangle$, (b) $\langle x_2 \rangle$, (c) $\langle x_3 \rangle$, (d) $\langle x_4 \rangle$ and 3D view of the phase space trajectory $\langle x_1 - x_2 - x_3 \rangle$, (e) classical result, (f) quantum result.

Adopting the values of all parameters $\hbar = 0.1$, $a = 1$, $b = 0.01$, $D = 6 \times 10^{-4}$. Here the stochastic variables η_1 and η_2 satisfying mean $M(\eta_1) = M(\eta_2) = 0$, variance $E(\eta_1) = E(\eta_2) = 0.001$. Comparisons of the results between classical-quantum system (7) and quantum system corresponding to Hamiltonian function (3) are conducted in Fig. 2, which present the conspicuous correspondence of the classical and quantum results, orange and blue lines represent the quantum and classical results, respectively. It can be seen that the trends of the trajectories of the classical-quantum system and the quantum system are very similar, with only small differences in mean amplitude. Furthermore, from the 3D view of the phase space, the two system behave similarly in terms of both shape and orbits [Figs. 2(e) and 2(f)]. Therefore, the dynamic properties of the quantum system can be uncovered by analyzing the dynamics of the classical-quantum system.

In addition to the simulation demonstration of similarity between the two systems, indeed, the quantum system becomes a classical Hamiltonian system in the limit $\hbar \rightarrow 0$ from the Schrödinger equation.

3. Force-based analysis of the classical-quantum system

The classical Hamiltonian system corresponding to the Hamiltonian function is

$$\begin{aligned} \dot{x}_1 &= \frac{\partial H}{\partial x_3} = x_3, & \dot{x}_2 &= \frac{\partial H}{\partial x_4} = x_4, \\ \dot{x}_3 &= -\frac{\partial H}{\partial x_1} = -ax_1x_2^2 - bx_1^3, \\ \dot{x}_4 &= -\frac{\partial H}{\partial x_2} = -ax_1^2x_2 - bx_2^3. \end{aligned} \quad (8)$$

The rate of change of $H(\mathbf{X})$ is

$$\dot{H}(\mathbf{X}) = \frac{dH(\mathbf{X})}{dt} = \nabla H(\mathbf{X})^T \dot{\mathbf{X}} = 0. \quad (9)$$

Therefore, the system is energy conserving. In addition, $V(t)$ is the phase-space volume, and the derivative of $V(t)$ is $\frac{dV(t)}{dt} = \nabla \cdot \mathbf{F} = \sum_{i=1}^n \frac{\partial f_i(\mathbf{X})}{\partial x_i} = 0$, and hence, in phase space, system (8) is an energy and volume-conserving system. The mechanical analysis includes performing a decomposition of the forces and determining the cycling of energy, and helps uncover the mechanism underlying the classical-quantum. System (7) written in vector form is

$$\dot{\mathbf{X}} = \begin{bmatrix} \dot{x}_1 \\ \dot{x}_2 \\ \dot{x}_3 \\ \dot{x}_4 \end{bmatrix} = \begin{bmatrix} x_3 \\ x_4 \\ -ax_1x_2^2 - bx_1^3 \\ -ax_1^2x_2 - bx_2^3 \end{bmatrix} + \begin{bmatrix} 0 \\ 0 \\ \sqrt{2D}\eta_1 \\ \sqrt{2D}\eta_2 \end{bmatrix}$$

$$\begin{aligned} &= \begin{bmatrix} 0 & 0 & 1 & 0 \\ 0 & 0 & 0 & 1 \\ -1 & 0 & 0 & 0 \\ 0 & -1 & 0 & 0 \end{bmatrix} \begin{bmatrix} ax_1x_2^2 + bx_1^3 \\ ax_1^2x_2 + bx_2^3 \\ x_3 \\ x_4 \end{bmatrix} + \begin{bmatrix} 0 \\ 0 \\ \sqrt{2D}\eta_1 \\ \sqrt{2D}\eta_2 \end{bmatrix} \\ &= \mathbf{J}(\mathbf{X}) \cdot \nabla H(\mathbf{X}) + \mathbf{R}, \end{aligned} \quad (10)$$

where the Hamiltonian energy, $H(\mathbf{X}) = K(\mathbf{X}) + U(\mathbf{X})$, comprises the kinetic energy $K(\mathbf{X})$ and potential energy $U(\mathbf{X})$, specifically,

$$K(\mathbf{X}) = \frac{1}{2}(x_3^2 + x_4^2), \quad (11)$$

$$U(\mathbf{X}) = \frac{a}{2}x_1^2x_2^2 + \frac{b}{4}(x_1^4 + x_2^4). \quad (12)$$

System (7) can also be transformed into an equivalent Kolmogorov-type system,

$$\begin{aligned} \dot{\mathbf{X}} &= \begin{bmatrix} \dot{x}_1 \\ \dot{x}_2 \\ \dot{x}_3 \\ \dot{x}_4 \end{bmatrix} = \begin{bmatrix} x_3 \\ x_4 \\ -ax_1x_2^2 - bx_1^3 \\ -ax_1^2x_2 - bx_2^3 \end{bmatrix} + \begin{bmatrix} 0 \\ 0 \\ \sqrt{2D}\eta_1 \\ \sqrt{2D}\eta_2 \end{bmatrix} \\ &= \begin{bmatrix} x_3 \\ x_4 \\ -x_1 \\ -x_2 \end{bmatrix} + \begin{bmatrix} 0 \\ 0 \\ x_1 - ax_1x_2^2 - bx_1^3 \\ x_2 - ax_1^2x_2 - bx_2^3 \end{bmatrix} + \begin{bmatrix} 0 \\ 0 \\ \sqrt{2D}\eta_1 \\ \sqrt{2D}\eta_2 \end{bmatrix} \\ &= \begin{bmatrix} 0 & 0 & 1 & 0 \\ 0 & 0 & 0 & 1 \\ -1 & 0 & 0 & 0 \\ 0 & -1 & 0 & 0 \end{bmatrix} \begin{bmatrix} x_1 \\ x_2 \\ x_3 \\ x_4 \end{bmatrix} \\ &\quad + \begin{bmatrix} 0 \\ 0 \\ x_1 - ax_1x_2^2 - bx_1^3 \\ x_2 - ax_1^2x_2 - bx_2^3 \end{bmatrix} + \begin{bmatrix} 0 \\ 0 \\ \sqrt{2D}\eta_1 \\ \sqrt{2D}\eta_2 \end{bmatrix} \\ &= \mathbf{J}(\mathbf{X}) \cdot \nabla H_1(\mathbf{X}) + \mathbf{E}(\mathbf{X}) + \mathbf{R}. \end{aligned} \quad (13)$$

Here we define a new Hamiltonian energy $H_1(\mathbf{X})$ as follows:

$$H_1(\mathbf{X}) = \frac{1}{2}(x_1^2 + x_2^2 + x_3^2 + x_4^2), \quad (14)$$

$$\nabla H_1(\mathbf{X}) = [x_1, x_2, x_3, x_4]^T, \quad (15)$$

with $H_1(\mathbf{X}) = K_1(\mathbf{X}) + U_1(\mathbf{X})$, a sum of the kinetic energy $K_1(\mathbf{X})$ and the potential energy $U_1(\mathbf{X})$, for which $K_1(\mathbf{X}) = \frac{1}{2}(x_3^2 + x_4^2)$, $U_1(\mathbf{X}) = \frac{1}{2}(x_1^2 + x_2^2)$. System (13) converts to

$$\begin{aligned} \dot{\mathbf{X}} &= \mathbf{J}(\mathbf{X}) \cdot \nabla H_1(\mathbf{X}) + \mathbf{E}(\mathbf{X}) + \mathbf{R} \\ &= \begin{bmatrix} 0 & 0 & 1 & 0 \\ 0 & 0 & 0 & 1 \\ -1 & 0 & 0 & 0 \\ 0 & -1 & 0 & 0 \end{bmatrix} \begin{bmatrix} 0 \\ 0 \\ x_3 \\ x_4 \end{bmatrix} + \begin{bmatrix} 0 & 0 & 1 & 0 \\ 0 & 0 & 0 & 1 \\ -1 & 0 & 0 & 0 \\ 0 & -1 & 0 & 0 \end{bmatrix} \begin{bmatrix} x_1 \\ x_2 \\ 0 \\ 0 \end{bmatrix} \\ &\quad + \begin{bmatrix} 0 \\ 0 \\ x_1 - ax_1x_2^2 - bx_1^3 \\ x_2 - ax_1^2x_2 - bx_2^3 \end{bmatrix} + \begin{bmatrix} 0 \\ 0 \\ \sqrt{2D}\eta_1 \\ \sqrt{2D}\eta_2 \end{bmatrix} \end{aligned}$$

$$= \mathbf{J}(\mathbf{X}) \cdot \nabla K_1(\mathbf{X}) + \mathbf{J}(\mathbf{X}) \cdot \nabla U_1(\mathbf{X}) + \mathbf{E}(\mathbf{X}) + \mathbf{R}. \quad (16)$$

In summary, systems (7), (10), (13), and (16) are equivalent systems.

Remark 1 (1) Similar to the three terms of the dissipative system, the three terms on the right-hand side of system (16) are understood as describing^[41] the inertial force (released by kinetic energy $K_1(\mathbf{X})$), the internal force (generated by potential energy $U_1(\mathbf{X})$), and the external force, including the dissipative force, produced by $\mathbf{E}(\mathbf{X}) + \mathbf{R}$.

(2) To the best of our knowledge, the literature contains no analysis of the mechanism underlying chaos production for a conservative system. The purpose behind transforming system (7) and system (8) into an equivalent dissipative Kolmogorov-type system is to unify the study of conservative chaos and dissipative systems, and to analyze the cause of chaos generation in classical-quantum system (7) and the classical Hamiltonian system (8).

The Casimir function, $C(\mathbf{X})$,^[38] is a very important physical quantity similar to the fluid dynamics studies. It is also meaningful in analyzing the system's stability and the global dynamics of the system. From the kernel of the Lie Poisson bracket, $C(\mathbf{X})$ is defined as^[47]

$$\{F(\mathbf{X}), G(\mathbf{X})\} = \mathbf{J}_{ik} \partial_i F \partial_k G = \nabla F(\mathbf{X})^T \mathbf{J} \nabla G(\mathbf{X}), \quad (17)$$

i.e., $\{C(\mathbf{X}), G(\mathbf{X})\} = 0, \forall G(\mathbf{X}) \in C^\infty(\mathfrak{g}^*)$. Hence, it represents a constant of the motion of the system (13), $\dot{C}(\mathbf{x}) = \{C(\mathbf{x}), H_1(\mathbf{x})\} = 0$. The Casimir function of system (13) has quadratic form

$$C(\mathbf{X}) = \frac{1}{2}(x_1^2 + x_2^2 + x_3^2 + x_4^2). \quad (18)$$

Definition The derivative of the Casimir function is called the Casimir power.

Considering the Casimir energy and Casimir power, from Refs. [38,40,41] we have:

- (1) If $\dot{C}(\mathbf{X}) > 0$ holds for all times, then the orbit of the system will diverge as a source.
- (2) If $\dot{C}(\mathbf{X})$ is a non-zero constant, i.e., $\dot{C}(\mathbf{X}) \equiv 0$ with $C(\mathbf{X}) \neq 0$, then the orbit will be periodic.
- (3) If $\dot{C}(\mathbf{X}) < 0$ holds for all times, then the orbit of the system will converge to a sink.
- (4) If $\dot{C}(\mathbf{X})$ oscillates periodically, then the orbit will be periodic.
- (5) If $\dot{C}(\mathbf{X})$ is bounded and irregularly vibrating around the zero line, then the orbit of the system will be chaotic.
- (6) If $\dot{C}(\mathbf{X})$ converges onto zero asymptotically, the orbit will converge to a sink.

Therefore, the Casimir power provides a criterion to determine whether a system can generate chaotic motion.

Next, we discuss the effects of the different types of forces on the system that alter its behavior from simplicity to complexity, and we reveal the key causes producing chaos. In the following, we set $a = 1$, $b = 0.01$, and impose the initial condition $\mathbf{X}_0 = [x_{10}, x_{20}, x_{30}, x_{40}]^T = [0.40, 0.60, 0.50, 0.414]^T$.

3.1. System containing only the conservative term

In this section, we mainly discuss the situation when the system contains inertial force $K_1(\mathbf{X})$, internal force $U_1(\mathbf{X})$ and part of external force $\mathbf{E}(\mathbf{X})$. At this time, the system is a Hamiltonian conservative system in any case.

3.1.1. System containing only the term of inertial force

When the system contains only the inertial force term (describing the kinetic energy released $K_1(\mathbf{X})$), i.e., $H_1(\mathbf{X}) = K_1(\mathbf{X}) = \frac{1}{2}(x_3^2 + x_4^2)$, the corresponding system is

$$\dot{\mathbf{X}} = \mathbf{J}(\mathbf{X}) \cdot \nabla K_1(\mathbf{X}) = \begin{bmatrix} 0 & 0 & 1 & 0 \\ 0 & 0 & 0 & 1 \\ -1 & 0 & 0 & 0 \\ 0 & -1 & 0 & 0 \end{bmatrix} \begin{bmatrix} 0 \\ 0 \\ x_3 \\ x_4 \end{bmatrix}. \quad (19)$$

As

$$\dot{H}_1(\mathbf{X}) = \dot{K}_1(\mathbf{X}) = x_3 \cdot \dot{x}_3 + x_4 \cdot \dot{x}_4 = 0, \quad (20)$$

system (19) is still a conservative system. Hence, $H_1(\mathbf{X}) = K_1(\mathbf{X}) = \text{constant}$ and $U_1(\mathbf{X}) = 0$, it is easy to prove that when the initial value is set to $\mathbf{X}_0 = [0.40, 0.60, 0.50, 0.414]^T$, then the Casimir power is

$$\begin{aligned} \dot{C}(\mathbf{X}) &= x_1 \cdot \dot{x}_1 + x_2 \cdot \dot{x}_2 + x_3 \cdot \dot{x}_3 + x_4 \cdot \dot{x}_4 \\ &= x_1 \cdot x_3 + x_2 \cdot x_4 > 0, \end{aligned} \quad (21)$$

and hence the trajectory diverges as a source [Fig. 3(a)]. The kinetic energy is conserved [Fig. 3(b)], and the Casimir energy increases with time [Fig. 3(c)]. The Casimir power is also greater than zero [Fig. 3(d)].

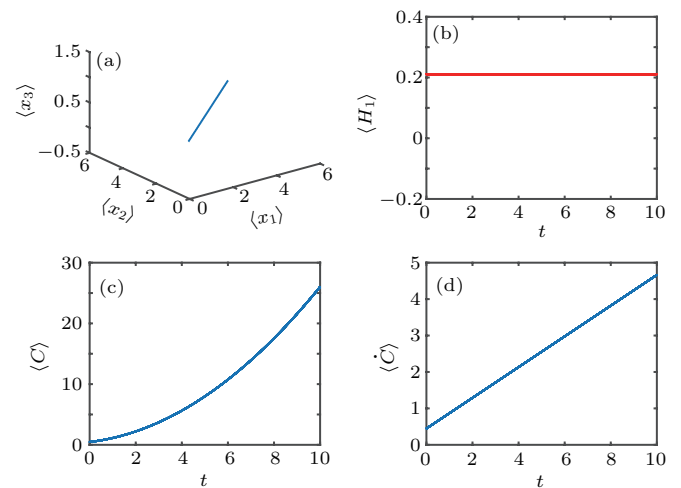


Fig. 3. System containing only the inertial force term, (a) 3D view of $\langle x_1 - x_2 - x_3 \rangle$. Time series of (b) the Hamiltonian energy $\langle H_1 \rangle$, (c) the Casimir energy, and (d) the Casimir power.

The reason why the Casimir energy of system (19) increases is that x_1 and x_2 are displacements. Although the momenta of the system, x_3 and x_4 , are conserved, the displacements x_1 and x_2 continue to increase, so the Casimir energy increases with the size of the displacements.

3.1.2. System containing both inertial and internal forces

When the system contains both inertial force (kinetic energy released $K_1(\mathbf{X})$) and internal force (potential energy stored $U_1(\mathbf{X})$), the governing equation becomes

$$\begin{aligned}\dot{\mathbf{X}} &= J(\mathbf{X}) \cdot \nabla H_1(\mathbf{X}) \\ &= J(\mathbf{X}) \cdot \nabla K_1(\mathbf{X}) + J(\mathbf{X}) \cdot \nabla U_1(\mathbf{X}) \\ &= \begin{bmatrix} 0 & 0 & 1 & 0 \\ 0 & 0 & 0 & 1 \\ -1 & 0 & 0 & 0 \\ 0 & -1 & 0 & 0 \end{bmatrix} \begin{bmatrix} 0 \\ 0 \\ x_3 \\ x_4 \end{bmatrix} + \begin{bmatrix} 0 & 0 & 1 & 0 \\ 0 & 0 & 0 & 1 \\ -1 & 0 & 0 & 0 \\ 0 & -1 & 0 & 0 \end{bmatrix} \begin{bmatrix} x_1 \\ x_2 \\ 0 \\ 0 \end{bmatrix} \\ &= \begin{bmatrix} 0 & 0 & 1 & 0 \\ 0 & 0 & 0 & 1 \\ -1 & 0 & 0 & 0 \\ 0 & -1 & 0 & 0 \end{bmatrix} \begin{bmatrix} x_1 \\ x_2 \\ x_3 \\ x_4 \end{bmatrix},\end{aligned}\quad (22)$$

and the rate of change of the Hamiltonian is $\dot{H}_1(\mathbf{X}) = \dot{K}_1(\mathbf{X}) + \dot{U}_1(\mathbf{X}) = 0$. The Hamiltonian for this system is also conservative. The rate of change of kinetic and potential energies are

$$\dot{K}_1(\mathbf{X}) = x_3 \cdot x_1 + x_4 \cdot x_2, \quad (23)$$

and

$$\dot{U}_1(\mathbf{X}) = -x_1 \cdot x_3 - x_2 \cdot x_4, \quad (24)$$

neither of which are conservative but exchange energy to conserve the total energy.

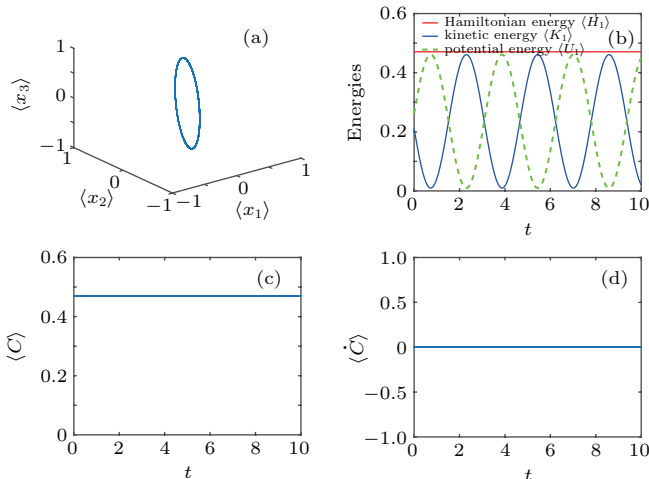


Fig. 4. System containing both inertial torque and internal force: (a) 3D view of $\langle x_1 - x_2 - x_3 \rangle$, (b) time series of energies, (c) time series of Casimir energy, (d) time series of Casimir power.

The Casimir power is

$$\begin{aligned}\dot{C}(\mathbf{X}) &= x_1 \cdot \dot{x}_1 + x_2 \cdot \dot{x}_2 + x_3 \cdot \dot{x}_3 + x_4 \cdot \dot{x}_4 \\ &= x_1 \cdot x_3 + x_2 \cdot x_4 - x_3 \cdot x_1 + x_4 \cdot x_2 = 0.\end{aligned}\quad (25)$$

Because both Casimir energy and Hamiltonian are conserved, the trajectory is a periodic orbit [Fig. 4(a)]. When kinetic energy increases, the potential energy decreases by an equal amount, thereby maintaining a constant energy [Fig. 4(b)]. The Casimir energy is constant [Fig. 4(c)] and the Casimir power is always zero [Fig. 4(d)], and thus reflects the observed conservation.

3.1.3. System containing containing inertial, internal forces and external force $E(\mathbf{X})$

Now, the system is governed by

$$\begin{aligned}\dot{\mathbf{X}} &= J(\mathbf{X}) \cdot \nabla K_1(\mathbf{X}) + J(\mathbf{X}) \cdot \nabla U_1(\mathbf{X}) + E(\mathbf{X}) \\ &= \begin{bmatrix} 0 & 0 & 1 & 0 \\ 0 & 0 & 0 & 1 \\ -1 & 0 & 0 & 0 \\ 0 & -1 & 0 & 0 \end{bmatrix} \begin{bmatrix} 0 \\ 0 \\ x_3 \\ x_4 \end{bmatrix} + \begin{bmatrix} 0 & 0 & 1 & 0 \\ 0 & 0 & 0 & 1 \\ -1 & 0 & 0 & 0 \\ 0 & -1 & 0 & 0 \end{bmatrix} \begin{bmatrix} x_1 \\ x_2 \\ 0 \\ 0 \end{bmatrix} \\ &\quad + \begin{bmatrix} 0 \\ 0 \\ x_1 - ax_1x_2^2 - bx_1^3 \\ x_2 - ax_1^2x_2 - bx_2^3 \end{bmatrix},\end{aligned}\quad (26)$$

which has a third term, an external force $E(\mathbf{X})$ but does not include the random variable part. System (26) is actually the original Hamiltonian system (8), so it is different from system (22). The external force changes the dynamic behavior from periodic trajectories of the previous system (22) [Fig. 4(a)] to chaotic orbits for system (26) [Fig. 5(a)], color represents the Casimir energy. Hence this external force is the important factor producing chaos.

The derivative of the Hamiltonian is $\dot{H}(\mathbf{X}) = \nabla H(\mathbf{X})^T \cdot J(\mathbf{X}) \cdot \nabla H(\mathbf{X}) = 0$, so $H(\mathbf{X})$ is conserved [Fig. 5(d)], but we notice that $H_1(\mathbf{X})$ changes [Fig. 5(c)]. From the perspective of $H_1(\mathbf{X})$ change, system (26) is similar to a dissipative system.

From system (26), the external force term $x_1 - ax_1x_2^2 - bx_1^3$ is present in the third equation, and $x_2 - ax_1^2x_2 - bx_2^3$ is present in the fourth equation. Both forces twist the system to produce chaos and both play complementary roles as either an external or dissipative force. The Casimir energy is irregular [Fig. 5(e)] and the Casimir power is

$$\begin{aligned}\dot{C}(\mathbf{X}) &= x_1\dot{x}_1 + x_2\dot{x}_2 + x_3\dot{x}_3 + x_4\dot{x}_4 \\ &= x_3x_1 + x_4x_2 - (bx_1^2 + ax_2^2)x_1x_3 - (ax_1^2 + bx_2^2)x_2x_4 \\ &= (1 - bx_1^2 - ax_2^2)x_1x_3 + (1 - ax_1^2 - bx_2^2)x_2x_4.\end{aligned}\quad (27)$$

Hence, the Casimir power decomposes into two terms

$$\dot{C}_{ex_3}(\mathbf{X}) = (1 - bx_1^2 - ax_2^2)x_1 \cdot x_3, \quad (28)$$

$$\dot{C}_{ex_4}(\mathbf{X}) = (1 - ax_1^2 - bx_2^2)x_2 \cdot x_4, \quad (29)$$

with

$$\dot{C}(\mathbf{X}) = \dot{C}_{ex3}(\mathbf{X}) + \dot{C}_{ex4}(\mathbf{X}). \quad (30)$$

Note that external force $x_1 - ax_1x_2^2 - bx_1^3$ of the third equation of system (26) is the source of the power factor $\dot{C}_{ex3}(\mathbf{X})$, and $x_2 - ax_1^2x_2 - bx_2^3$ of the fourth equation contributes to the power factor $\dot{C}_{ex4}(\mathbf{X})$. Hence, we can have the following conclusions.

Remark 2 The Casimir power of system (26) does not depend on the inertial or internal force, but on external forces. The two components of the Casimir power undergo mutual exchanges.

We need to demonstrate how the two external forces, $x_1 - ax_1x_2^2 - bx_1^3$ and $x_2 - ax_1^2x_2 - bx_2^3$ in Eq. (26), play both applying and dissipative roles. In Fig. 5(f), the curve in the first line corresponds to the term $\dot{C}_{ex3}(\mathbf{X})$ of the Casimir power. In some time intervals, it is positively indicating that the external force $x_1 - ax_1x_2^2 - bx_1^3$ accelerates the system and supplies energy. However, in other time intervals, it is negatively indicating that the same external $x_1 - ax_1x_2^2 - bx_1^3$ decelerates the system and expends energy. The same argument applies to $\dot{C}_{ex4}(\mathbf{X})$ as for $\dot{C}_{ex3}(\mathbf{X})$ [Fig. 5(f), second line]. Therefore, the two external forces are indistinguishable in their action on the system. The sum $\dot{C}_{ex3}(\mathbf{X}) + \dot{C}_{ex4}(\mathbf{X})$ represents the exchange power [Fig. 5(f), third line].

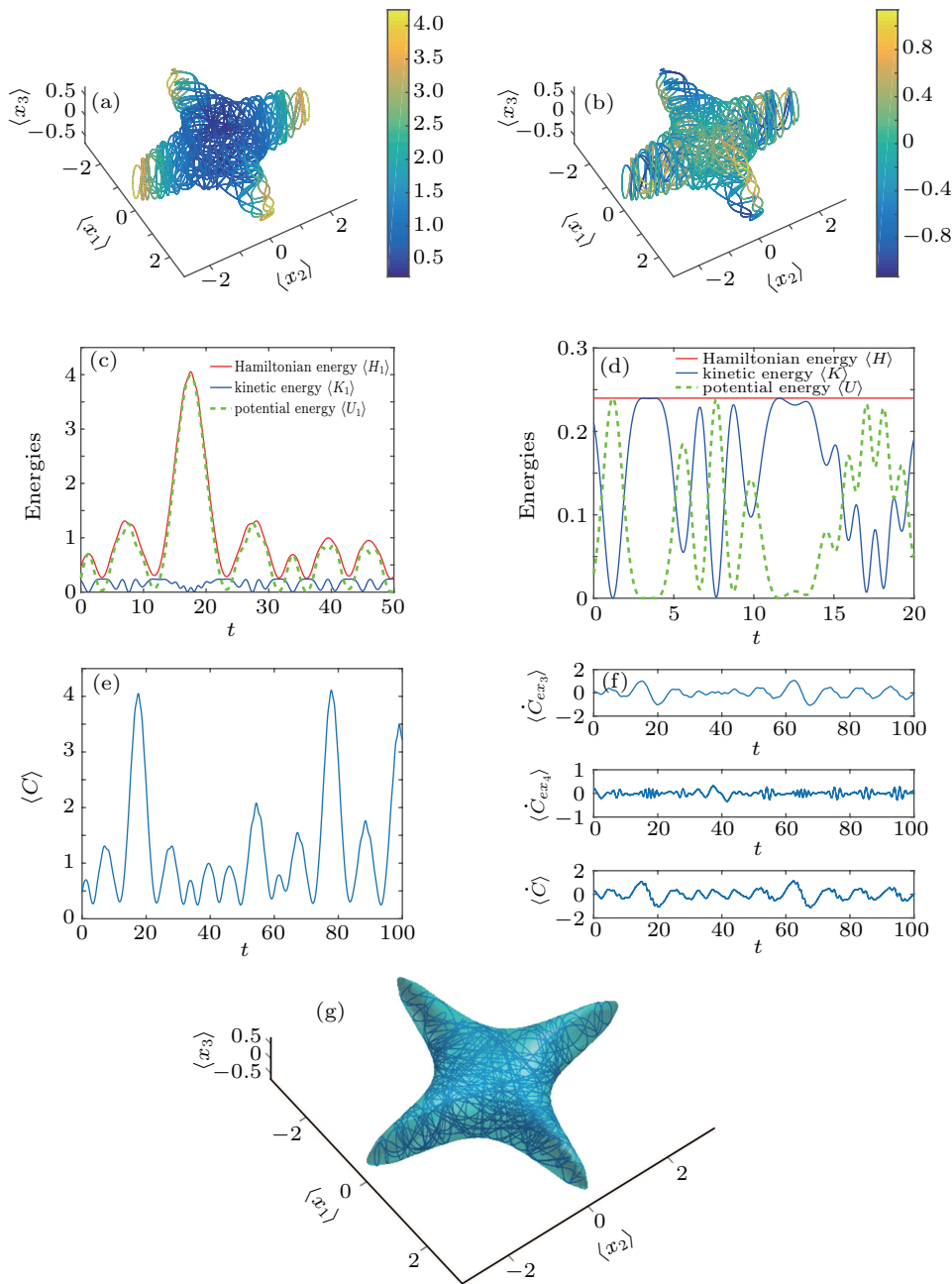


Fig. 5. Conservative Hamiltonian system containing all three forces producing chaos: 3D view of the phase space trajectory $\langle x_1 - x_2 - x_3 \rangle$ with (a) Casimir energy (color scale) and (b) Casimir power. Time series of (c) and (d) energies, (e) Casimir energy, and (f) Casimir power. (g) The chaotic orbit and supremum hypersurface bound.

The Casimir power $\dot{C}(\mathbf{X})$ oscillates irregularly around the zero line and is bounded, thus further evidencing the chaotic nature of the trajectory of the system [Fig. 5(f)]. Figures 5(a) and 5(b) show two orbits along with a color coding of the Casimir energy and Casimir power, respectively. Note that both energy and power dictate the trajectories of the chaotic system.

In general, the bounds of a chaotic system are difficult to find, especially in an analytic form. Nevertheless, we find an analytic bound for the chaotic trajectory of this conservative Hamiltonian.

Theorem 1 The classical Hamiltonian system (8) has supremum bound

$$H(\mathbf{X}) = \frac{1}{2}(x_3^2 + x_4^2) + \frac{a}{2}x_1^2x_2^2 + \frac{b}{4}(x_1^4 + x_2^4) = H_0, \quad (31)$$

where H_0 is the initial value of $H(\mathbf{X})$.

Proof Because the Hamiltonian $H(t) = H_0$ is valid for any time, Equation (31) constitutes the supremum hypersurface bound. The proof is completed.

In Fig. 5(g), the orbits are completely and exactly enclosed within the blue-green transparent supremum surface bound. Note that the figure shows a 3D figure in the phase space $x_1 - x_2 - x_3$, so H_0 can be evaluated by any point in this figure, i.e., $H_0 = \frac{1}{2}x_{30}^2 + \frac{a}{2}x_{10}^2x_{20}^2 + \frac{b}{4}(x_{10}^4 + x_{20}^4)$.

Remark 3 (1) The original conservative Hamiltonian system (8) is transformed into an equivalent Kolmogorov system. The dynamical mechanical analysis used to analyze the dissipative system is employed to analyze the dynamics of the conservative system. This method reveals the causes of chaos in the conservative system very well and it provides a link between the dissipative and conservative systems.

(2) When $H(\mathbf{X})$ is constant, there is no way to explain the system dynamics using the Hamiltonian, the Casimir energy however changes and is able to explain the energy exchange. Therefore, the Casimir power can analyze the dynamic characteristics of the system. That is, the Hamiltonian and Casimir functions both complement each other, and using them, we can determine the characteristics of the system.

(3) The Kolmogorov–Arnold–Moser (KAM) theorem is a well-known result for understanding the Hamiltonian chaotic systems.^[48] From the KAM theory, if a Hamiltonian system having function H_1 is perturbed by another Hamiltonian system having function H_2 , then the coupled Hamiltonian system with function $H = H_1 + \varepsilon H_2$ may produce chaos because the two Hamiltonian systems exchange energy. However, the KAM theory must use a coupled system to analyze a system, it is unable to analyze why the system is chaotic from the system itself when only a single Hamiltonian exists. In the above description, we convert the Hamiltonian system into a dissipative-like system and analyze why the system produces

chaos through the force decomposition. Compared with the KAM theory, this method provides a new perspective and is convenient.

Let Lyapunov exponents of the system are L_1, L_2, L_3, L_4 , respectively, and $L_1 \geq L_2 \geq L_3 \geq L_4$.

(a) Setting $b = 0.01$ and $\mathbf{X}_0 = [0.40, 0.60, 0.50, 0.414]^T$ while varying a , we find that if $a \in [0, 0.035]$ we obtain $L_1 = L_2 = L_3 = L_4 = 0$, and hence the classical Hamiltonian system (8) performs periodic or quasi-periodic dynamics [Fig. 6(a)]. If $a \in (0.035, 2]$, $L_1 > 0, L_2 = L_3 = 0$, and $L_4 = -L_1 < 0$, system (7) undergoes chaotic flow.

The Lyapunov exponents are symmetric about the zero point [Fig. 6], and the sum of Lyapunov exponents is equal to zero, further verifying that the system is conservative.

(b) Setting $a = 1$ and initial value $\mathbf{X}_0 = [0.40, 0.60, 0.50, 0.414]^T$ while varying b , the Lyapunov exponents of the classical Hamiltonian system (8) are calculated [Fig. 6(b)]. For $b \in [0, 0.21]$, we obtain $L_1 > 0, L_2 = L_3 = 0$, and $L_4 = -L_1 < 0$, hence the classical Hamiltonian system (8) exhibits conservative chaos. For $b \in (0.21, 2]$, we obtain $L_1 = L_2 = L_3 = L_4 = 0$, and hence system (8) performs periodic or quasi-periodic motion.

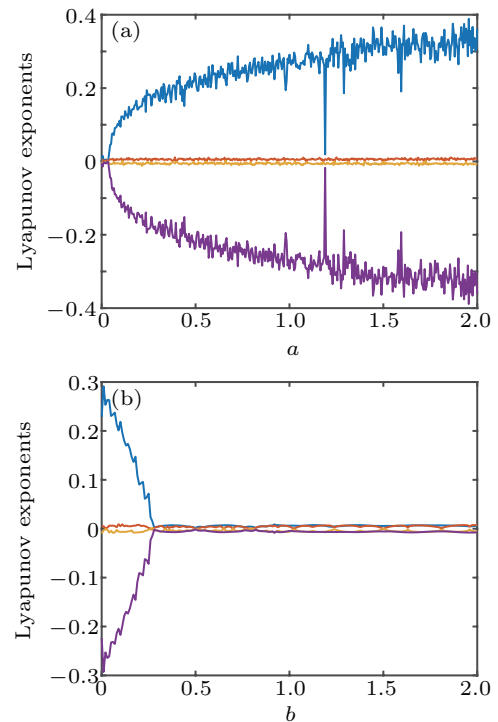


Fig. 6. Lyapunov exponent of system (8) at $\mathbf{X}_0 = [0.40, 0.60, 0.50, 0.414]^T$: (a) varying a with $b = 0.01$, (b) varying b with $a = 1$.

3.2. System containing both the term of conservative and random variables

When the system contains the terms of inertial, internal, external force and random variables \mathbf{R} , the governing equation turns into

$$\dot{\mathbf{X}} = \mathbf{J}(\mathbf{X}) \cdot \nabla H_1(\mathbf{X}) + \mathbf{E}(\mathbf{X}) + \mathbf{R}$$

$$\begin{aligned}
 &= \begin{bmatrix} 0 & 0 & 1 & 0 \\ 0 & 0 & 0 & 1 \\ -1 & 0 & 0 & 0 \\ 0 & -1 & 0 & 0 \end{bmatrix} \begin{bmatrix} 0 \\ 0 \\ x_3 \\ x_4 \end{bmatrix} + \begin{bmatrix} 0 & 0 & 1 & 0 \\ 0 & 0 & 0 & 1 \\ -1 & 0 & 0 & 0 \\ 0 & -1 & 0 & 0 \end{bmatrix} \begin{bmatrix} x_1 \\ x_2 \\ 0 \\ 0 \end{bmatrix} \\
 &+ \begin{bmatrix} 0 \\ 0 \\ x_1 - ax_1x_2^2 - bx_1^3 \\ x_2 - ax_1^2x_2 - bx_2^3 \end{bmatrix} + \begin{bmatrix} 0 \\ 0 \\ \sqrt{2D}\eta_1 \\ \sqrt{2D}\eta_2 \end{bmatrix} \\
 &= \mathbf{J}(\mathbf{X}) \cdot \nabla K_1(\mathbf{X}) + \mathbf{J}(\mathbf{X}) \cdot \nabla U_1(\mathbf{X}) + \mathbf{E}(\mathbf{X}) + \mathbf{R}. \quad (32)
 \end{aligned}$$

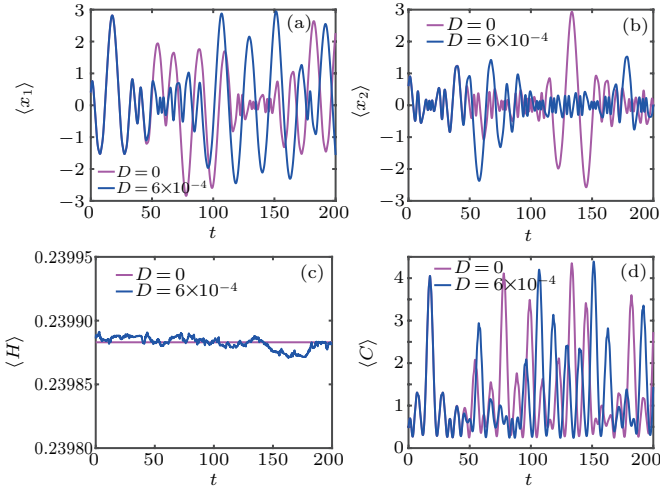


Fig. 7. Time series (a) $\langle x_1 \rangle$, (b) $\langle x_2 \rangle$, (c) Hamiltonian energy, and (d) Casimir energy.

System (32) is actually the original classical-quantum system (7). In Fig. 7, blue and purple lines represent the results of system (7) and system (8), respectively, which indicates that the orbits of two systems diversify after a period of time. Actually,

in terms of Hamiltonian energies of the two systems, they only differ a little bit [Fig. 7(c)]. However, Casimir energy changes greatly, which reveals the reason why the large difference of trajectories of the two systems [Figs. 7(a) and 7(b)]. Due to the addition of random variables, the trajectory of system (7) varies greatly. This also explains why there is large decoherence between quantum system and the classical Hamiltonian system (8),^[12] but the quantum-classical systems have a good correspondence.

4. Energies of classical-quantum correspondence

In this section, quantum-classical correspondence is further revealed via comparing energies. In Fig. 8, blue curves represent the classical-quantum behaviors produced by system (7), purple curves stand for the quantum results produced by system (2) with Wigner function (3). The quantum-classical correspondence of phase portrait in $x_1 - x_2$ is verified in Fig. 8(a). Figures 8(b), 8(c) and 8(d) display quantum-classical correspondence of kinetic energy, potential energy and Casimir energy, respectively. The amplitudes of kinetic energy and Casimir energy of the two systems are not much different. However, amplitudes of the potential energy of the two systems differ greatly. The reason should be that the potential energy contains quartic terms. The energy determines the dynamics of a system, therefore analysis combining all energies helps to comprehend the correspondence and difference between the two systems.

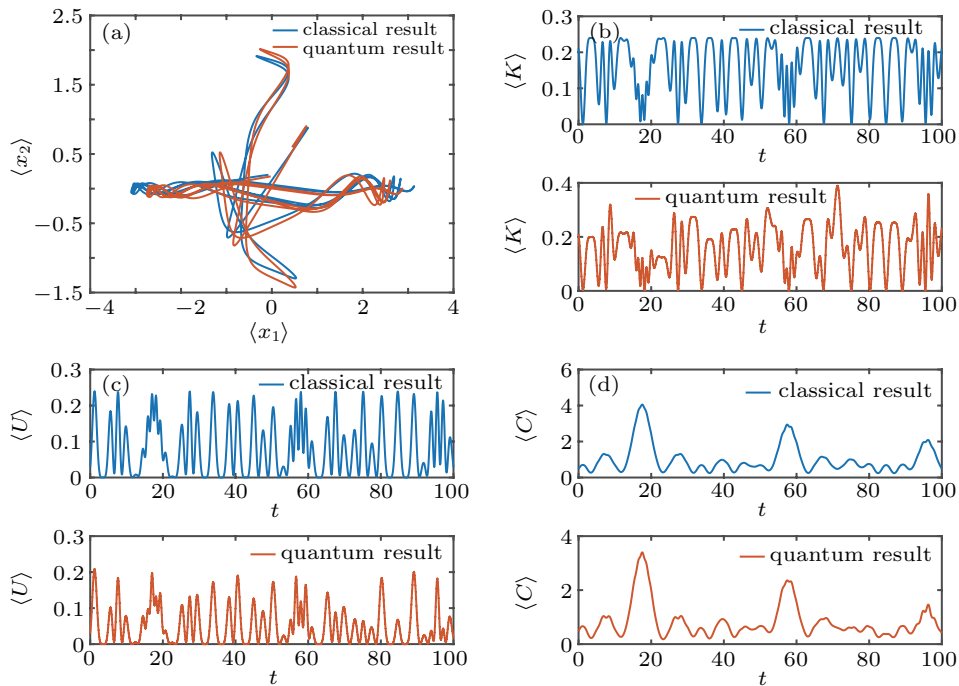


Fig. 8. Quantum-classical correspondence, (a) phase portrait for the $\langle x_1 - x_2 \rangle$, (b) the kinetic energy $\langle K \rangle$, (c) the potential energy $\langle U \rangle$, (d) the Casimir energy $\langle C \rangle$.

5. Conclusions

Quantum-classical correspondence has been conducted via the Wigner function and a classical-quantum chaotic system containing random variables. A dynamic mechanical analysis has been used effectively in analyzing a classical-quantum system exhibiting strongly chaotic flow. The system is transformed into an equivalent Kolmogorov-type system. The vector field of the chaotic Hamiltonian system is decomposed into three different forces. We find that combinations of different forces (or different energies) determine the dynamical behaviors of the system, such as periodic orbits. The Casimir energy and power are effective in finding insights into causes of different dynamical behaviors produced. For the corresponding classical Hamiltonian system, the supremum bound of the system is analytically derived and verified, and rich dynamics of the system are explored through the Lyapunov spectrum. Differences between the classical quantum system and the classical Hamiltonian system are displayed by trajectories and energies. Quantum-classical correspondences are further demonstrated by comparing phase portrait, energies of the two systems.

Acknowledgment

We thank Dr. Richard Haase at Edanz Group China (www.liwenbianji.cn/ac) for editing the English text of a draft of this manuscript.

References

- [1] Averin D V 2000 *Fortschritte der Physik* **48** 1055
- [2] Houck A A, Türeci H E and Koch J 2012 *Nat. Phys.* **8** 292
- [3] Xia H Y, Li H S, Zhang H, Liang Y and Xin J 2019 *Quantum Inf. Process.* **18** 229
- [4] Sheng Y B and Zhou L 2013 *Entropy* **15** 1776
- [5] Zabaleta O G and Arizmendi C M 2018 *Chaos* **28** 075506
- [6] Wilkie J and Brumer P 1997 *Phys. Rev.* **55** 43
- [7] Brack M, Bhaduri R K, Law J and Murthy M V N 1993 *Phys. Rev. Lett.* **70** 568
- [8] Hou X W and Hu B 2004 *Phys. Rev. A* **69** 042110
- [9] Song L J, Wang X G, Yan D and Zong Z G 2008 *Int. J. Theor. Phys.* **47** 2635
- [10] Song L J, Yan D, Gai Y J and Wang Y B 2011 *Acta. Phys. Sin.* **60** 073201 (in Chinese)
- [11] Eckhardt B, Hose G and Pollak E 1989 *Phys. Rev. A* **39** 3776
- [12] Gong J and Brumer P 1999 *Phys. Rev. E* **60** 1643
- [13] Gong J and Brumer P 2003 *Phys. Rev. A* **68** 062103
- [14] Qi G Y, Hu J B and Wang Z 2020 *Appl. Math. Model.* **78** 350
- [15] Lakshmanan M and Rajasekar S 2012 *Nonlinear Dynamics- Integrability, Chaos, and Patterns* (Berlin: Springer-Verlag) chap 3 p. 65
- [16] Taylor J R 2005 *Classical mechanics* (Sausalito: University Science Books) chap 13 p. 543
- [17] Shi L J and Wen Z S 2019 *Chin. Phys. B* **28** 040201
- [18] Shen J, Zhang X M, Li Q L, Wang X Y, Zhao Y J and Jia Y 2019 *Chin. Phys. B* **28** 040503
- [19] Alamodi A O A, Sun K H, Ai W, Chen C and Peng D 2019 *Chin. Phys. B* **28** 020503
- [20] Song N, Zhang W and Yao M H 2015 *Nonlinear Dyn.* **82** 489
- [21] Xiang L, Jia Y and Hu A 2016 *Appl. Math. Model.* **40** 1
- [22] Wei Z C and Zhang W 2014 *Int. J. Bifurc. Chaos* **24** 1450127
- [23] Wei Z C, Zhang W and Yao M H 2015 *Nonlinear Dyn.* **82** 1251
- [24] Bi H Y, Qi G Y and Hu J B 2019 *Complexity* **6313925**
- [25] Zhang X and Wang C H 2019 *IEEE Access* **7** 16336
- [26] Zhang X, Wang C H, Yao W and Lin H R 2019 *Nonlinear Dyn.* **97** 2159
- [27] Deng Q L and Wang C H 2019 *Int. J. Bifurc. Chaos* **29** 1950117
- [28] Xu Y, Gu R, Zhang H and Li D 2012 *Int. J. Bifurcat. Chaos* **22** 1250088
- [29] Yao M H, Zhang W and Zu W J 2012 *J. Sound Vib.* **331** 2624
- [30] Wei Z C, Moroz I, Sprott J C, Wang Z and Zhang W 2017 *Int. J. Bifurc. Chaos* **27** 1730008
- [31] Zhang W, Wu Q L, Yao M H and Dowell E H 2018 *Nonlinear Dynam.* **94** 1
- [32] Wu Q L, Zhang W and Dowell E H 2018 *Int. J. Non-Lin. Mech.* **102** 25
- [33] Wu Q L and Qi G Y 2019 *Phys. Lett. A* **383** 1555
- [34] Deng Q L and Wang C H 2019 *Chaos* **29** 093112
- [35] Qi G Y 2019 *Nonlinear Dynam.* **95** 2063
- [36] El-Sayed A M A, Nour H M, Elsaid A, Matouk A E and Elsonbaty A 2016 *Appl. Math. Model.* **40** 3516
- [37] Pelino V, Maimone F and Pasini A 2014 *Chaos Soliton Fract.* **64** 67
- [38] Qi G Y 2017 *Appl. Math. Model.* **51** 686
- [39] Qi G Y and Hu J B 2017 *Int. J. Bifurcat. Chaos* **27** 1750216
- [40] Yang Y J and Qi G Y 2017 *Chaos Soliton Fract.* **108** 187
- [41] Qi G Y and Liang X Y 2017 *Int. J. Bifurcat. Chaos* **27** 1750180
- [42] Qi G Y and Zhang J F 2017 *Chaos Soliton Fract.* **99** 7
- [43] Liang X Y and Qi G Y 2017 *Chaos Soliton Fract.* **98** 173
- [44] Liang X Y and Qi G Y 2017 *Brazil J. Phys.* **47** 288
- [45] Yang Y J and Qi G Y 2019 *Phys. Lett. A* **383** 318
- [46] Boulet B 2006 *Fundamentals of Signals and Systems* (Boston: Charles River Media) chap 5 p. 188
- [47] Marsden J E and Ratiu T S 2010 *Introduction to mechanics and symmetry: a basic exposition of classical mechanical systems* (New York, Springer) chap 1 p. 35
- [48] Shamolin M V 2010 *J. Math. Sci.* **165** 743